

# Thermal Conductivity of Carbon Fiber/Liquid Crystal Polymer Composites

Jason M. Keith, Julia A. King, Michael G. Miller, Amanda M. Tomson

Department of Chemical Engineering, Michigan Technological University, Houghton, Michigan 49931-1295

Received 16 June 2006; accepted 19 July 2006

DOI 10.1002/app.25102

Published online in Wiley InterScience (www.interscience.wiley.com).

**ABSTRACT:** Thermally conductive resins are needed for bipolar plates in fuel cells. Currently, the materials used for these bipolar plates often contain a single type of graphite in a thermosetting resin. In this study, varying amounts of two different types of polyacrylonitrile based carbon fibers, Fortafil 243 and Panex 30, were added to a thermoplastic matrix (Vectra A950RX Liquid Crystal Polymer). The resulting single filler composites were tested for thermal conductivity and a simple exponential thermal conductivity model was developed for the square root of the product of the in-plane and through-plane thermal conductivity  $\sqrt{k_{in}k_{out}}$ . The experiments showed that the through-plane thermal conductivity was similar for composites up to 40 vol % fiber. However, at higher loadings, the Panex 30 samples

exhibited higher thermal conductivity. The experiments also showed that the in-plane thermal conductivity of composites containing Panex 30 was higher than those containing Fortafil 243 for all volume fractions studied. Finally, the model agreed very well with experimental data covering a large range of filler volume fraction (from 0 to 55 vol % for both single filler systems). The model can be used with existing through-plane thermal conductivity models to predict in-plane thermal conductivity. © 2006 Wiley Periodicals, Inc. *J Appl Polym Sci* 102: 5456–5462, 2006

**Key words:** composites; fillers; liquid crystalline polymers; extrusion; thermal properties

## INTRODUCTION

Most polymer resins are thermally insulating. Increasing the thermal conductivity of these resins allows them to be used in other applications. One emerging market for thermally conductive resins is for bipolar plates for use in fuel cells. The bipolar plate separates one cell from the next, with this plate carrying hydrogen gas on one side and air (oxygen) on the other side. Bipolar plates require high thermal conductivity (to conduct heat), low gas permeability, and good dimensional stability.

Typical thermal conductivity values for some common materials are 0.2–0.3 for polymers, 234 for aluminum, 400 for copper, and 600 for graphite (all values in W/m (K)). One approach to improving the thermal conductivity of a polymer is through the addition of a conductive filler material, such as carbon and metal. Con-

ductive resins with a thermal conductivity from  $\sim 1$  to 30 W/m K can be used in heat sink applications.<sup>1</sup>

A significant amount of work has been conducted varying the amount of single conductive fillers in a composite material.<sup>2–9</sup> For example, ceramic fibers/particles (boron nitride, aluminum nitride, and aluminum oxide), metal fibers/particles (aluminum, steel, iron, copper, and silver), and Ni-coated glass fibers have been used.<sup>3,10–13</sup> Metallic fillers have several disadvantages, relative to carbon, which include higher density and greater susceptibility to oxidation. Various types of carbons have been effective conductive fillers. For example, synthetic graphite particles and carbon fibers are often added to polymers to increase the composite thermal conductivity.<sup>7,9,10,14,15</sup>

In this project, researchers performed compounding runs followed by injection molding of carbon fiber/liquid crystal polymer (LCP) test specimens. Varying amounts of two different types of polyacrylonitrile (PAN) based carbon fiber (Fortafil 243 and Panex 30) were added to Vectra A950RX LCP. The resulting single fiber composites were then tested for thermal conductivity. Recently, a new analytical technique has been developed to measure thermal conductivities of isotropic and anisotropic materials.<sup>16–20</sup> The goal of this research was to develop a simple empirical model for the in-plane thermal conductivity using this new analytical technique. Although the technical literature has extensive experimental and modeling data for

Correspondence to: J. A. King (jaking@mtu.edu).

Contract grant sponsor: Department of Energy, Michigan Technological University; contract grant number: DE-FG02-04ER63821.

Contract grant sponsor: National Science Foundation; contract grant number: DMI-0456537.

Contract grant sponsor: Graduate Assistance in Areas of National Need, U.S. Department of Education; contract grant number: P200A030192.

TABLE I  
Properties of Ticona's Vectra A950RX<sup>25</sup>

Melting point	280°C
Tensile modulus (1 mm/min)	10.6 GPa
Tensile stress at break (5 mm/min)	182 MPa
Tensile strain at break (5 mm/min)	3.4%
Flexural modulus at 23°C	9.1 GPa
Notched izod impact strength at 23°C	95 KJ/m <sup>2</sup>
Density at 23°C	1.40 g/cc
Volumetric electrical conductivity at 23°C	10 <sup>-16</sup> S/cm
Surface electrical conductivity	10 <sup>-14</sup> S
Thermal conductivity at 23°C	0.2 W/m K (approx.)
Humidity absorption (23°C/50% RH)	0.03 wt %
Mold shrinkage (parallel)	0.0%
Mold shrinkage (normal)	0.7%
Coefficient of linear thermal expansion (parallel)	0.04 × 10 <sup>-4</sup> °C <sup>-1</sup>
Coefficient of linear thermal expansion (normal)	0.38 × 10 <sup>-4</sup> °C <sup>-1</sup>

through-plane thermal conductivity,<sup>27-28</sup> there is little reported data for the in-plane thermal conductivity.

## MATERIALS AND METHODS

### Materials

The matrix used for this project was Ticona's Vectra A950RX Liquid Crystal Polymer (LCP), which is a highly ordered thermoplastic copolymer consisting of 73 mol % hydroxybenzoic acid and 27 mol % hydroxynaphtholic acid. This LCP has the properties needed for bipolar plates, namely high dimensional stability up to a temperature of 250°C, extremely short molding times (often 5-10 s), exceptional dimensional reproducibility, chemically resistant in acidic environments present in a fuel cell, and a low hydrogen gas permeation rate.<sup>25,26</sup> The properties of this polymer are shown in Table I.<sup>25</sup>

The first carbon fiber used in this study was Fortafil 243, now sold by Toho Tenax America. Fortafil 243 is a

TABLE II  
Properties of Fortafil 243 Carbon Fiber<sup>27</sup>

Carbon content	95 wt %
Electrical resistivity	0.00167 ohm cm
Thermal conductivity	20 W/m K (axial direction)
Tensile strength	3600 MPa
Tensile modulus	227 GPa
Specific gravity	1.74 g/cc
Fiber diameter	7.5 µm
Fiber shape	Round
Fiber mean length	3.2 mm (entire range is 2.3-4.1mm)
Binder content	2.6 wt % proprietary polymer that adheres pellet together and promotes adhesion with nylon matrix
Bulk density	356 g/L

TABLE III  
Properties of Panex 30 MF Milled High Purity Carbon Fiber<sup>28</sup>

Carbon content	99.5 wt %
Electrical resistivity	0.0014 ohm cm
Thermal conductivity	22 W/m K (axial direction, approximate)
Tensile strength	3600 MPa
Tensile modulus	207 GPa
Specific gravity	1.75 g/cc
Fiber diameter	7.4 µm
Fiber shape	Round
Fiber mean length	150 µm
Bulk density	445 g/L

polyacrylonitrile (PAN) based 3.2 mm chopped and pelletized carbon fiber was used to improve the electrical and thermal conductivity and the tensile strength of the resin. Fortafil 243 was surface treated and then formed into pellets. A proprietary polymer (sizing) is used as a binder for the pellets that also promotes adhesion with the matrix. Table II shows the properties of this carbon fiber, which is 95 wt % carbon.<sup>27</sup>

Table III shows the properties of Zoltek's Panex 30 MF milled 150-µm long high purity carbon fiber. This carbon fiber is PAN based and is electrochemically surface treated but not sized. Panex 30 is produced by a high temperature batch graphitization process that produces fiber that is 99.5 wt % carbon.<sup>28</sup>

Thermal conductivity was measured on composites containing varying amounts of these carbon fibers in Vectra A950RX. The concentrations (shown in wt % and the corresponding vol %) for these single filler composites are shown in Tables IV and V.

### Test specimen fabrication

For this entire project, the fillers were used as-received. Vectra A950RX was dried in an indirect heated

TABLE IV  
Single Filler Loading Levels of Fortafil 243 in Vectra

Fiber (wt %)	Fiber (vol %)
0.0	0.0
5	4.1
7.5	6.1
10	8.2
15	12.4
20	16.6
25	21.2
30	25.5
35	30.2
40	34.9
45	39.7
50	44.6
55	49.6
60	54.7

TABLE V  
Single Filler Loading Levels of Panex 30 in Vectra

Fiber (wt %)	Fiber (vol %)
0.0	0.0
5	4.0
7.5	6.1
10	8.2
15	12.4
20	16.7
25	21.1
30	25.5
35	30.1
40	34.8
45	39.9
50	44.4
55	49.4
60	54.5

dehumidifying drying oven at 150°C and then stored in moisture barrier bags.

The extruder used was an American Leistritz Extruder Corp. Model ZSE 27. This extruder has a 27 mm corotating intermeshing twin screw with 10 zones and a length/diameter ratio of 40. The screw design used is shown elsewhere.<sup>29</sup> The screw design was chosen to allow a large concentration of filler to mix with the matrix material and thereby achieve the maximum possible conductivity. The Vectra polymer pellets were introduced in Zone 1. A side stuffer located at Zone 5 was used to introduce the carbon fibers into the polymer melt. Two Schenck AccuRate gravimetric feeders were used to accurately control the amount of each material added to the extruder.

After passing through the extruder, the composite strands (3 mm in diameter) entered a water bath and then a pelletizer that produced nominally 3 mm long pellets. After compounding, the pelletized composite resin was dried again and then stored in moisture barrier bags prior to injection molding.

A Nigata injection molding machine, model NE85UA<sub>4</sub>, was used to produce test specimens. This machine has a 40 mm diameter single screw with a length/diameter ratio of 18. The lengths of the feed, compression, and metering sections of the single screw are 396, 180, and 144 mm, respectively. A four cavity mold was used to produce 6.4 cm diameter disks (end gated). The thermal conductivity of all formulations was determined. Prior to conducting the conductivity tests, the samples were conditioned at 23°C and 50% RH for 88 h and then tested.<sup>30</sup>

#### Fiber length and orientation test method

To determine the length of the carbon fiber in the molded test specimens, diethylenetriamine was used to dissolve the matrix. The fibers were then dispersed onto a glass slide and viewed using an Olympus SZH10 optical microscope with an Optronics Engi-

neering LX-750 video camera. Additional details of this method are shown elsewhere.<sup>31</sup>

To determine the orientation of the carbon fiber, a polished composite sample was viewed using an optical microscope. For the through-plane thermal conductivity samples, the center portion was cut out of a disk and set in epoxy such that the through the sample thickness (3.2 mm) face could be viewed. The samples were then polished and viewed using an Olympus BX60 reflected light microscope. More details of this test method are shown elsewhere.<sup>31</sup>

#### Through-plane thermal conductivity test method

The through-plane thermal conductivity of a 3.2 mm thick, 5 cm diameter disc-shaped test specimen was measured at 55°C using a Holometrix Model TCA-300 Thermal Conductivity Analyzer according to the ASTM F433 guarded heat flow meter method.<sup>32</sup> For each formulation, six samples were tested.

#### Transient plane source thermal conductivity test method and theory

The Mathis Instruments Hot Disk Thermal Constants Analyzer is an emerging technology that can measure the in-plane and through-plane thermal conductivity of an anisotropic material in the same test, using the transient plane source technique.<sup>16-20</sup> The sensor used in this test method consisted of a 10 µm thick nickel foil embedded between two 25.4-µm thick layers of Kapton polyimide film. The nickel foil was wound in a double spiral pattern with a radius *R* of 3.189 mm. The thermal conductivities were measured at 23°C.

Figure 1 shows how the sensor is positioned between two samples of composite material. In this

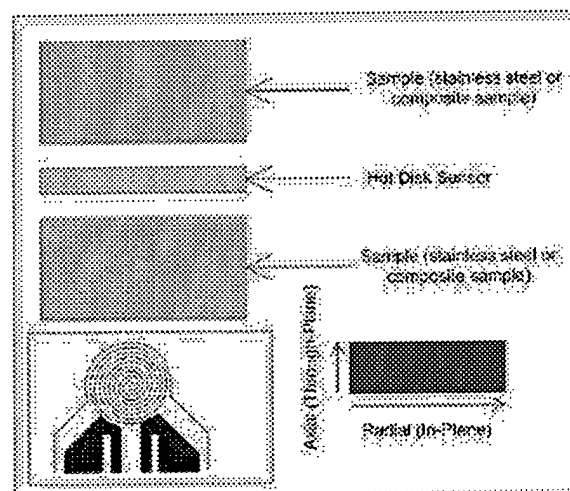


Figure 1. Schematic of samples and sensor for hot disk. The insert at the lower left shows the double spiral heating element.

experiment, the samples tested were composite disks of diameter  $D = 63.5$  mm and thickness  $T = 3.18$  mm. To help ensure that the assumption of an infinite sample domain was met and that heat was not penetrating completely through the sample in the axial direction, two of these composite disks were stacked together above the sensor and two more stacked below it, giving us a double thickness of sample. This stacking of disks allowed the generation of more reproducible data. For each formulation, typically 5 different sets of 4 disks (so a total of 20 disks) were tested.

The sensor then had a constant electrical power (variable by sample from 0.25 to 0.80 W) over a short period of time (variable by sample from 5 to 40 s) passed through. The generated heat dissipated within the double spiral was conducted through the kapton insulating layer and into the surrounding sample, causing a rise in the temperature of the sensor and the sample.

From a theoretical standpoint, the double spiral pattern can be approximated to a series of concentric, equally spaced ring sources. The characteristic heat conduction equation, assuming radial symmetry in the sample, is then given as:

$$(\rho C_p) \frac{\partial T}{\partial t} = k_m \frac{1}{r} \left( \frac{\partial}{\partial r} \left( r \frac{\partial T}{\partial r} \right) \right) + k_{thru} \frac{\partial^2 T}{\partial z^2} + \sum_{\text{rings}} Q_i \delta(r - r') \delta(z) \quad (1)$$

where  $\rho$  is the density of the sample ( $\text{kg/m}^3$ ),  $C_p$  is the heat capacity of the sample ( $\text{J/kg K}$ ),  $T$  is the temperature of the sample ( $\text{K}$ ),  $t$  is the time of the measurement (s),  $k_m$  and  $k_{thru}$  are the in-plane and through-plane thermal conductivities of the sample ( $\text{W/m K}$ ),  $\delta$  is the Dirac  $\delta$  function,  $r'$  is the radius of one of the ring sources, and  $Q_i$  is the power supplied to that ring

per unit length of the ring ( $\text{W/m}$ ). The total power for each ring is proportional to the circumference of the ring  $2\pi r'$ , such that the total power supplied for all of the rings is  $Q$  (W). This total power  $Q$  is an input parameter to the Hot Disk Thermal Constants Analyser. The first term in eq. (1) represents accumulation of thermal energy, the second term radial (referred to as in-plane in our experiments) heat conduction, the third term axial (referred to as through-plane in our experiments) heat conduction, and the final term is a heat source.

The sample can be approximated as an infinite domain if the experimental time is much less than the characteristic thermal diffusion time. For an anisotropic material in a cylindrical geometry, the experimental time must meet the following two criteria:  $t \ll (D/2)^2/(\alpha_m)$  and  $t \ll T^2/(\alpha_{thru})$ . In these formulas,  $\alpha = k/(\rho C_p)$ , which is the thermal diffusivity of the composite material.

The average transient temperature increase of the sensor is simultaneously measured by recording the change in electrical resistance of the nickel sensor<sup>16-20</sup> according to

$$\Delta T = \frac{1}{\beta} \left( \frac{R_n}{R_{n0}} - 1 \right) \quad (2)$$

where  $\Delta T$  is the change in temperature at time  $t$  ( $\text{K}$ ),  $\beta$  is the temperature coefficient of resistance of the material ( $1/\text{K}$ ),  $R_n$  is the electrical resistance of the nickel at time  $t$  ( $\Omega$ ), and  $R_{n0}$  is the electrical resistance of the nickel at time 0 ( $\Omega$ ). The temperature rise in eq. (2) is correlated with the in-plane and through-plane thermal conductivities through the solution of eq. (1) as

$$\Delta T = \frac{P}{\pi^{3/2} R \sqrt{k_m k_{thru}}} F(\tau) \quad (3)$$

TABLE VI  
Thermal Conductivity Results for Composites Containing Fortafil 243 Carbon Fiber

Formulation (wt %)	Through-plane thermal conductivity (TCA-300) ( $\text{W/m K}$ )	Through-plane thermal conductivity (hot disk) ( $\text{W/m K}$ )	In-plane thermal conductivity (hot disk) ( $\text{W/m K}$ )	In-plane to through-plane ratio (hot disk) (unitless)
Neat Vectra A950RX LCP	0.217 $\pm$ 0.007 ( $n = 4$ )	~ 0.22 (TCA)	~ 0.22 (TCA)	N/A
Fortafil 243 Carbon Fiber				
5	0.237 $\pm$ 0.006 ( $n = 6$ )	0.238 $\pm$ 0.002 ( $n = 5$ )	1.143 $\pm$ 0.030 ( $n = 5$ )	4.8
7.5	0.256 $\pm$ 0.004 ( $n = 6$ )	0.255 $\pm$ 0.002 ( $n = 5$ )	1.205 $\pm$ 0.034 ( $n = 5$ )	4.7
10	0.272 $\pm$ 0.006 ( $n = 6$ )	0.271 $\pm$ 0.005 ( $n = 5$ )	1.234 $\pm$ 0.052 ( $n = 5$ )	4.6
15	0.282 $\pm$ 0.006 ( $n = 6$ )	0.282 $\pm$ 0.004 ( $n = 5$ )	1.407 $\pm$ 0.012 ( $n = 5$ )	5.0
20	0.316 $\pm$ 0.007 ( $n = 6$ )	0.320 $\pm$ 0.004 ( $n = 5$ )	1.543 $\pm$ 0.026 ( $n = 5$ )	4.8
25	0.352 $\pm$ 0.006 ( $n = 6$ )	0.353 $\pm$ 0.001 ( $n = 5$ )	1.680 $\pm$ 0.026 ( $n = 5$ )	4.8
30	0.366 $\pm$ 0.009 ( $n = 5$ )	0.365 $\pm$ 0.003 ( $n = 5$ )	1.857 $\pm$ 0.028 ( $n = 5$ )	5.1
35	0.430 $\pm$ 0.025 ( $n = 6$ )	0.432 $\pm$ 0.004 ( $n = 5$ )	1.996 $\pm$ 0.005 ( $n = 5$ )	4.6
40	0.527 $\pm$ 0.014 ( $n = 6$ )	0.527 $\pm$ 0.003 ( $n = 5$ )	2.050 $\pm$ 0.036 ( $n = 5$ )	3.9
45	0.599 $\pm$ 0.033 ( $n = 6$ )	0.602 $\pm$ 0.006 ( $n = 5$ )	2.109 $\pm$ 0.015 ( $n = 5$ )	3.5
50	0.687 $\pm$ 0.034 ( $n = 4$ )	0.688 $\pm$ 0.004 ( $n = 5$ )	2.239 $\pm$ 0.037 ( $n = 5$ )	3.3
55	0.836 $\pm$ 0.050 ( $n = 5$ )	0.838 $\pm$ 0.009 ( $n = 20$ )	2.324 $\pm$ 0.069 ( $n = 20$ )	2.8
60	1.039 $\pm$ 0.018 ( $n = 5$ )	1.030 $\pm$ 0.023 ( $n = 10$ )	2.459 $\pm$ 0.057 ( $n = 10$ )	2.4

TABLE VII  
Thermal Conductivity Results for Composites Containing Panex 30 Carbon Fiber

Formulation (wt %)	Through-plane thermal conductivity (TCA-300) (W/m K)	Through-plane thermal conductivity (hot disk) (W/m K)	In-plane thermal conductivity (hot disk) (W/m K)	In-plane to through-plane ratio (hot disk) (unitless)
Neat Vectra A950RX LCP	0.217 ± 0.007 (n = 4)	~ 0.22 (TCA)	~ 0.22 (TCA)	N/A
Panex 30 Carbon Fiber				
5	0.238 ± 0.005 (n = 6)	0.238 ± 0.001 (n = 5)	1.270 ± 0.010 (n = 5)	5.3
7.5	0.260 ± 0.006 (n = 5)	0.261 ± 0.001 (n = 5)	1.304 ± 0.007 (n = 5)	5.0
10	0.276 ± 0.003 (n = 4)	0.277 ± 0.002 (n = 5)	1.414 ± 0.013 (n = 5)	5.1
15	0.281 ± 0.006 (n = 4)	0.281 ± 0.002 (n = 5)	1.736 ± 0.012 (n = 5)	6.2
20	0.318 ± 0.009 (n = 5)	0.319 ± 0.002 (n = 5)	1.988 ± 0.011 (n = 5)	6.2
25	0.339 ± 0.007 (n = 6)	0.334 ± 0.002 (n = 5)	2.385 ± 0.030 (n = 5)	7.1
30	0.360 ± 0.017 (n = 6)	0.377 ± 0.002 (n = 5)	2.600 ± 0.015 (n = 5)	6.9
35	0.459 ± 0.016 (n = 6)	0.455 ± 0.006 (n = 5)	2.888 ± 0.017 (n = 5)	6.3
40	0.524 ± 0.009 (n = 5)	0.528 ± 0.005 (n = 5)	3.137 ± 0.016 (n = 5)	5.9
45	0.630 ± 0.009 (n = 4)	0.592 ± 0.008 (n = 5)	3.376 ± 0.094 (n = 5)	5.7
50	0.663 ± 0.013 (n = 6)	0.860 ± 0.020 (n = 5)	3.559 ± 0.051 (n = 5)	4.1
55	1.036 ± 0.007 (n = 4)	1.035 ± 0.004 (n = 5)	3.852 ± 0.042 (n = 5)	3.7
60	1.264 ± 0.022 (n = 5)	1.264 ± 0.001 (n = 5)	4.109 ± 0.013 (n = 5)	3.3

where  $F(\tau)$  is a dimensionless time dependent function of  $\tau = \sqrt{\alpha_{\text{eff}} t} / R^2$  given by an integral of a double series over the number of rings  $m$

$$F(\tau) = [m(m+1)]^{-2} \int_0^\tau \sigma^{-2} \left[ \sum_{l=1}^m l \sum_{k=1}^m k \exp\left(-\frac{l^2 + k^2}{4m^2\sigma^2}\right) I_0\left(\frac{lk}{2m^2\sigma^2}\right) \right] d\sigma \quad (4)$$

A more detailed derivation of eqs. (3) and (4) is given by He.<sup>33</sup>

## RESULTS

### Fiber length and orientation results

For the molded test specimens containing both carbon fibers, the fiber length was typically 70  $\mu\text{m}$ . The corresponding fiber aspect ratio (length/diameter) was 9. As shown previously for the through-plane thermal conductivity samples, the fibers are primarily oriented transverse to the conductivity measurement direction. Photomicrographs are shown elsewhere.<sup>24</sup>

### Thermal conductivity results

Tables VI and VII display the thermal conductivity results (mean, standard deviation, and number of samples tested) using both thermal conductivity test methods for the samples containing Fortafil 243 and Panex 30, respectively. The through-plane thermal conductivities  $k_{\text{thp}}$  are similar for both the TCA-300 and HotDisk and are shown as a function of volume fraction  $\phi$  in Figure 2. The conductivities are about the same for each filler, but at higher loading levels the Panex 30 composites exhibit higher thermal conductivity. The in-plane thermal conductivities  $k_{\text{in}}$  are

shown as a function of filler volume fraction  $\phi$  in Figure 3. Composites containing Panex 30 have higher thermal conductivity for all filler loading levels. This is also verified with the higher ratio of in-plane to through-plane thermal conductivities as listed in Tables VI and VII. Panex/Vectra composites likely have higher thermal conductivity because of the higher thermal conductivity of the constituent Panex 30 fiber as compared to the Fortafil 243 fiber (Tables II and III). For composites containing 50–60 wt % carbon fiber, the through-plane thermal conductivity is ~20% higher for the Panex composites. This is higher than the 10% higher thermal conductivity of the Panex 30 fiber (22 W/m K) as compared to Fortafil 243 fiber (20 W/m K). This observation could imply that the thermal conductivity of the constituent Panex 30 is actually higher than the 22 W/m K value estimated by the vendor.

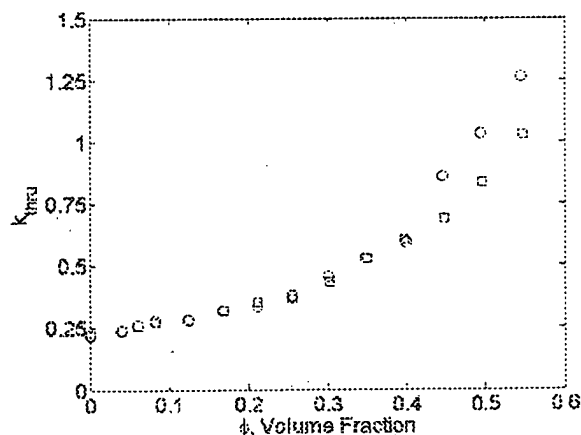


Figure 2 Through-plane thermal conductivities (W/m K) for composites containing Fortafil 243 (squares) and Panex 30 (circles) carbon fiber.

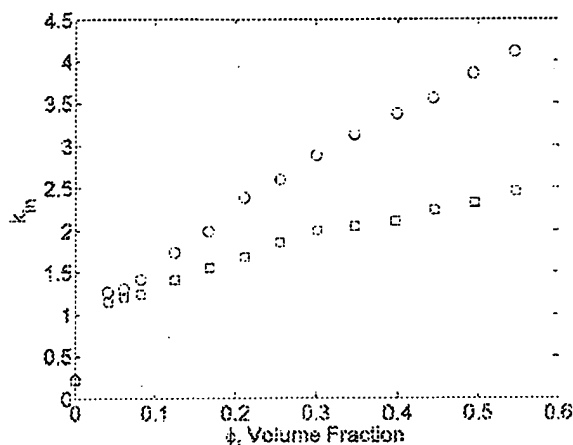


Figure 3 In-plane thermal conductivities (W/m K) for composites containing Fortafil 243 (squares) and Panex 30 (circles) carbon fiber.

It was desired to develop a simple model for the in-plane thermal conductivity  $k_{in}$  using the results in Tables VI and VII. The work of Keith et al.<sup>34</sup> developed a linear correlation between the square root of the product of the in-plane and through-plane conductivities  $\sqrt{k_{in}k_{thru}}$  with the filler volume fraction  $\phi$ . This was for nylon composites containing one of two single fillers: synthetic graphite or carbon fiber at relatively low loading (up to 40 wt %). The work of Miller et al.<sup>35</sup> showed that at higher loading levels (up to 75 wt %), Vectra composites containing synthetic graphite exhibits an exponential dependence of  $\sqrt{k_{in}k_{thru}}$  with  $\phi$ . This correlation can be used for the present work for Vectra/Fortafil 243 carbon fiber composites as:

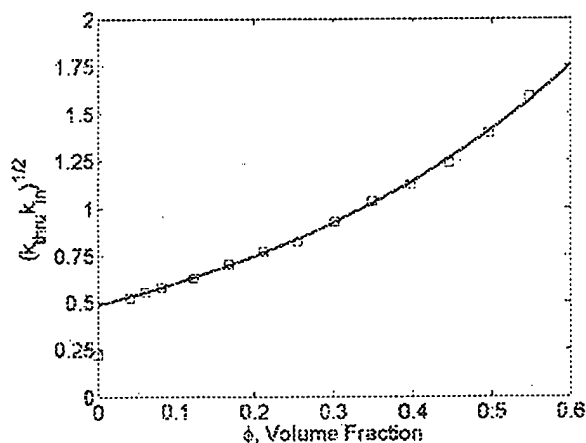


Figure 4 Square root of the product of through-plane and in-plane thermal conductivities for composites containing Fortafil 243 carbon fiber. Data points are squares and a model fit is given by the solid line.

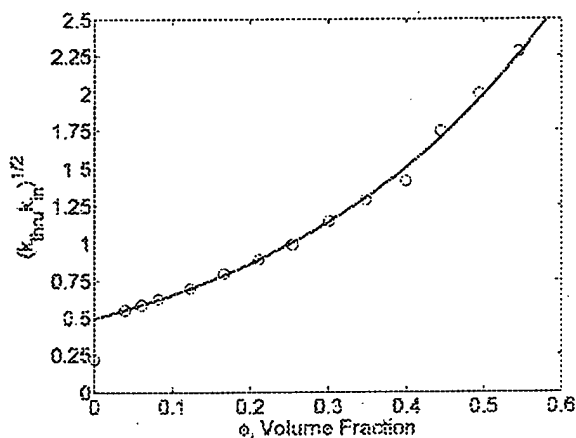


Figure 5 Square root of the product of through-plane and in-plane thermal conductivities for composites containing Panex 30 carbon fiber. Data points are circles and a model fit is given by the solid line.

$$\sqrt{k_{in}k_{thru}} = 0.4841 e^{2.1478\phi} \quad (5)$$

as seen in Figure 4 and for Vectra/Panex 30 carbon fiber composites as

$$\sqrt{k_{in}k_{thru}} = 0.4927 e^{2.7933\phi} \quad (6)$$

as seen in Figure 5. It is noted that in eqs. (5) and (6), all thermal conductivities must have units of (W/m K). Two generalizations can be made when comparing with the Vectra/synthetic graphite correlation (given as  $\sqrt{k_{in}k_{thru}} = 0.4633 e^{4.9256\phi}$  by Miller et al.<sup>35</sup>). First of all, the pre-exponential factor is nearly the same for all formulations with an average value of 0.48 W/m K. Second, the exponent for synthetic graphite is much larger indicating a significantly larger effect on the composite thermal conductivity, when compared to the carbon fiber composites.

## CONCLUSIONS

In this project, two different carbon fibers (Fortafil 243 and Panex 30) were tested for thermal conductivity at single filler loadings of up to 60 wt % (55 vol %) in Vectra A950RX LCP. Through-plane and in-plane thermal conductivities were measured. The Panex 30 composites exhibited higher in-plane thermal conductivity over the entire range of fillers studied. These composites also showed improved through-plane thermal conductivity at filler loadings above 40 vol %. At lower loadings the through-plane thermal conductivities were identical.

A simple exponential model for the square root of the product of the in-plane and through-plane thermal conductivities  $\sqrt{k_{in}k_{thru}}$  was also developed. The results showed outstanding agreement with the ex-

perimental data. This model can be combined with through-plane thermal conductivity models from the literature to predict the in-plane thermal conductivity.

The authors gratefully thank the American Leistritz technical staff for recommending an extruder screw design. The authors also thank the following undergraduate students for their assistance on this project: Kara Lenhart, Terrence Mazure, Stephanie Natrass, Troy Tambling, Elaine Venema, and Amanda Zalud.

## References

- Finan, J. M. In *Proceedings of the Society of Plastics Engineers Annual Technical Conference*, New York, 1999; p 1547.
- Agari, Y.; Uno, T. *J Appl Polym Sci* 1985, 30, 2225.
- Bigg, D. M. *Polym Eng Sci* 1977, 17, 842.
- Bigg, D. M. *Adv Polym Technol* 1984, 4, 255.
- Narkis, M.; Lidor, G.; Vaxman, A.; Zuri, L. *J Electrostat* 1999, 47, 201.
- Nagata, K.; Iwabuchi, H.; Nigo, H. *Compos Interfaces* 1999, 6, 483.
- Demain, A. Ph.D. Dissertation, Université Catholique de Louvain, Louvain-la-Neuve, Belgium, 1994.
- King, J. A.; Tucker, K. W.; Meyers, J. D.; Weber, E. H.; Clingerman, M. L.; Ambrosius, K. R. *Polym Compos* 2001, 22, 142.
- Murthy, M. V. In *Proceedings of the Society of Plastics Engineers Annual Technical Conference*, New York, 1994; p 1396.
- Taipalus, R.; Harnia, T.; Zhang, M. Q.; Friedrich, K. *Compos Sci Technol* 2001, 61, 861.
- Sunon, R. M. *Polym News* 1985, 11, 102.
- Maplestone, P. *Mod Plast* 1992, 69, 60.
- Bigg, D. M. *Polym Compos* 1986, 7, 125.
- Brosius, B. *High Performance Compos* 2001, 22, (September/October).
- Thengguang, W.; Spontak, B. J.; Balik, C. M. *Polymer* 2002, 43, 3717.
- Gustavsson, M.; Karawacki, E.; Gustafsson, S. E. *Rev Sci Instrum* 1994, 65, 3856.
- Log, T.; Gustafsson, S. E. *Fire Mater* 1995, 19, 43.
- Bohac, V.; Gustavsson, M. K.; Kubicar, L.; Gustafsson, S. E. *Rev Sci Instrum* 2003, 71, 2452.
- Hot Disk Thermal Constants Analyzer Instruction Manual; Mathis Instruments: Fredericton, New Brunswick, Canada, 2001.
- Transient Plane Source-Gustafsson Hot Disk Technique, Standards for Contact Transient Measurements of Thermal Properties, National Physical Laboratory, United Kingdom. Available at <http://www.npl.co.uk/thermal/ctm> (last accessed on June 2006).
- Weber, E. H. Ph.D. Dissertation, Michigan Technological University, Houghton, MI, 2001.
- Weber, E. H.; Clingerman, M. L.; King, J. A. *J Appl Polym Sci* 2003, 88, 112.
- Weber, E. H.; Clingerman, M. L.; King, J. A. *J Appl Polym Sci* 2003, 88, 123.
- Heiser, J. A.; King, J. A. *Polym Compos* 2004, 25, 186.
- Ticona Vectra liquid crystal polymer (LCP) product information. Ticona, Summit, NJ, 2000.
- Chieu, J. S.; Paul, D. R. *J Polym Sci Part B: Polym Phys* 1987, 25, 1699.
- Fortafil Carbon Fibers Technical Data Sheet, Toho Tenax America, Inc., 121 Cardiff Valley Road, Rockwood, TN.
- Zoltek Panex Carbon Fibers Technical Data Sheet, 3101 McKelvey Road, St. Louis, MO.
- King, J. A.; Keith, J. M.; Smith, R. C.; Morrison, F. A. *Polym Compos*, in press.
- Plastics-Standard Atmospheres for Conditioning and Testing, ISO 291:1997, ISO, Switzerland, 1998.
- Heiser, J. A.; King, J. A.; Konell, J. P.; Suttler, L. L. *Polym Compos* 2004, 25, 407.
- Standard Test Methods for Evaluating Thermal Conductivity of Gasket Materials, ASTM Standard E430-77 (Reapproved 1993), ASTM, Philadelphia, 1998.
- He, Y. *Thermochim Acta* 2005, 436, 122.
- Keith, J. M.; Hingst, C. D.; Miller, M. G.; King, J. A.; Hauser, R. A. *Polym Compos* 2006, 27, 1.
- Miller, M. G.; Keith, J. M.; King, J. A.; Edwards, B. J.; Klinkenberg, N.; Schiraldi, D. A. *Polym Compos* 2006, 27, 388.